Food Hydrocolloids 82 (2018) 45–52

Contents lists available at ScienceDirect

Food Hydrocolloids

journal homepage: www.elsevier.com/locate/foodhyd

Survival of *Saccharomyces cerevisiae* microencapsulated with complex coacervate after freezing process

A. de la Cruz-Gavia [a], C. Pérez-Alonso [a], C.E. Barrera-Díaz [a], J. Alvarez-Ramírez [b], H. Carrillo-Navas [b], A.Y. Guadarrama-Lezama [a, *]

[a] Facultad de Química, Universidad Autónoma del Estado de México, Paseo Colón esq. Paseo Tollocan s/n, Col. Residencial Colón, Toluca, Estado de México, 50120, Mexico

[b] Departamento de Ingeniería de Procesos e Hidráulica, Universidad Autónoma Metropolitana-Iztapalapa, San Rafael Atlixco No. 186, Col. Vicentina, Ciudad de México, 09340, Mexico

ARTICLE INFO

Article history:
Available online 26 March 2018

Keywords:
Saccharomyces cerevisiae
Complex coacervate
Zeta potential
Microencapsulation
Freezing process
Yeast survival

ABSTRACT

Complex coacervate from whey protein isolate (WPI)-*Saccharomyces cerevisiae* (Y) was prepared for microencapsulation by spray-drying. The optimum WPI-Y complex coacervate reached the best interaction for a ratio and pH of 1:13 and 3.28, respectively. The complex coacervate was spray-dried with 10% and 20% w/w of total solids content using maltodextrin DE10 (MD) as wall material and subsequently frozen at −18 °C. DSC, FTIR and SEM analyses were carried out to characterize thermal, chemical and structural properties of pure materials and spray-dried WPI-Y complex coacervates. Thermograms of DSC reflected that the spray-dried WPI-Y complex coacervates were better protected when MD concentration increased because the denaturation peak temperature of proteins and enthalpy were higher. These results were confirmed with FTIR analysis since peaks intensity of amino groups was highest in the spray-dried WPI-Y complex coacervate containing 20% w/w of total solids content. After the freezing process, reduced decrease in the peaks intensity of the amides in the spray-dried WPI-Y complex coacervate with 20% w/w of total solids content was observed. Morphology of all spray-dried complex coacervates exhibited particles of spherical shapes with concavities, dents and hollows in the center. However, particles after the freezing process displayed fractures in the surface. Finally, yeast survival was higher in the spray-dried WPI-Y complex coacervate with higher concentration of MD and as well after freezing process. Therefore, WPI-Y complex coacervates were stable after freezing process and can be used to stabilize fermentative microorganisms in order to produce frozen dough with similar characteristics that the dough.

1. Introduction

Freezing is a process widely used for large-scale production of dough and bread. Freezing offers several advantages, including reduced costs of dough production, easy handling and large-scale dough storage and distribution. However, storage of frozen dough is not free of quality deterioration problems (Bot, 2003; Ribotta, Pérez, Leon, & Anon, 2004; Rosell & Gómez, 2007; Selomulyo & Zhou, 2007). Loss of dough strength is induced by reduction of cross-linking as caused by water migration and distribution in the dough microstructure, as well as to ice re-crystallization (Giannou, Kessoglou, & Tzia, 2003; Räsänen, Blanshard, Mitchell, Derbyshire, & Autio, 1998). A second major problem relates to the reduction in gassing capacity caused by decline in activity and viability of yeast. As consequence, the effective storage time of dough intended for bread production can be drastically reduced. Fixing the problems related to loss of dough strength and decline of gassing power should lead to longer storage times while preserving dough textural and rheological properties.

Different additives have been proposed to retain quality and freshness of frozen dough in the bakery industry. For instance, mono- and diacetyltartaric acid and guar gum have shown to improve texture and volume of bread fabricated from frozen dough, although rheological parameters were not improved (Ribotta et al., 2004). Vegetable shortening and emulsifiers have also beneficial effects in textural characteristics of frozen dough (Kim, Huang, Du,

* Corresponding author.
E-mail address: ayguadarramal@uaemex.mx (A.Y. Guadarrama-Lezama).

https://doi.org/10.1016/j.foodhyd.2018.03.045
0268-005X/

Pan, & Chung, 2008; Matuda, Parra, Lugao, & Tadini, 2005). Oat proteins offer anti-freeze effects, lowering freezable water in dough matrix (Zhang, Zhang, Wang, Qian, & Qi, 2015). Mixtures of sodium alginate and xanthan gum have been also explored, showing improvements in the quality of bread from frozen dough (Kondakci, Ang, & Zhou, 2015).

The problem of preserving the functionality and activity of yeast during frozen storage is a challenging issue. Relatively long storage periods can lead to severe reduction of yeast strains, and hence to deteriorated quality of bread made from frozen dough. Microencapsulation is a technologically viable approach for protecting yeast strains from adverse effects of long periods of frozen storage (Đorđević et al., 2015). Colloidosomes have been explored as vehicles for yeast cell encapsulation, offering acceptable capacity to metabolize glucose from solution, although diffusive transport restrictions were detected (Keen, Slater, & Routh, 2011). Layer-by-layer assembly of chitosan and carboxymethil cellulose was explored, showing enhanced cell survival under adverse pH and temperature conditions (Priya, Vijayalakshmi, & Raichur, 2011). It has been shown that corn starch and maltodextrin used as carrier materials for spray-drying can lead to acceptable results with respect to cell survival (approx. 85%) (Chandralekha et al., 2016). Complex coacervation is also a viable alternative for encapsulation of active cells (Bosnea, Moschakis, & Biliaderis, 2017; Eghbal & Choudhary, 2018). Complex coacervation process is a liquid-liquid phase separation phenomenon that usually occurs when electrostatic interactions are established between oppositely charged biopolymers are brought together under certain specific conditions (Timilsena, Wang, Adhikari, & Adhikari, 2017). Coacervation of whey protein isolate and gum Arabic has shown to preserve *L. paracasei* for relatively long time (about 45 days) (Bosnea et al., 2017).

The use of complex coacervates from protein and polysaccharides for yeast preservation in frozen dough has been poorly explored. In this regard, the aims of this work were a) to design a complex coacervate system to encapsulate Y using complex coacervate and MD as wall material; b) to evaluate the survival from Y after freezing process.

2. Materials and methods

2.1. Materials

Dry yeast (*Saccharomyces cerevisiae,* Y in short) for baker purposes was acquired from Nevada brand (Safmex S.A. de C.V., Toluca, Mexico). The yeasts count of Y was 30×10^7 CFU/g. Whey protein isolate (WPI) was obtained from Hilmar Ingredients (Hilmar, CA, USA). Maltodextrin DE10 (MD) was purchased from Sigma Aldrich (St. Louis, MO, USA). Hydrochloric acid (HCl), sodium hydroxide (NaOH) and sodium chlorite (NaCl) were purchased from J.T. Baker (Xalostoc, State of Mexico, Mexico). Potato dextrose agar and sterile saline peptone water were acquired from BD Bioxon brand (Becton, Dickinson and Company, Cuautitlán Izcalli, Mexico). All reagents were analytical grade. Deionized water was used for the preparation of all solutions.

2.2. WPI and Y solutions and complex coacervate preparation

In a first step, stock dispersions of WPI and Y were prepared, which will be used for complex coacervation. WPI (1.0% w/w) and Y (0.1% w/w) solutions were prepared by dispersing powders in deionized water and dispersed under gently continuous magnetic stirring during 24 h to ensure complete hydration of the materials at pH 6.76 and 4.63, respectively (Poirier, Maréchal, Richard, & Gervais, 1999). The pH of the WPI solution was adjusted at pH 3.0 with HCl solution (0.1 M). Then, Y solution (0.1% w/w) was slowly added to the solution of WPI to obtain WPI-Y complex coacervate.

2.3. Zeta potential measurements

Complex coacervation is given by electrostatic interaction between cationic and anionic materials. Zeta potential is a proxy of the electrostatic charges carried out by biomaterials. The accurate measurement of zeta potential provides a framework to conduct cation-anion like neutralization interactions, which eventually lead to complex coacervate formation. Zeta potential measurements were determined with Zetasizer Nano Z (Malvern Instruments Ltd., Worcestershire, UK). The pH of the WPI and Y solutions (20 mL) was adjusted by adding HCl or NaOH solution (0.1 M) from 2.0 to 10.0, every 1.0 unit at 25 °C to determine the behavior of the materials. The effect of the interaction of WPI-Y complex coacervate in the zeta potential was obtained by varying the mass ratio ranging from 1:1 to 1:20. The mean value of the zeta potential was obtained from the equipment software.

2.4. Turbidity measurements

In principle, complex coacervation can take place over a wide range of conditions. A common approach to assess the formation of complex coacervation is via the turbidity induced by insoluble complexes. In this way, turbidity measurements were performed of WPI-Y complex coacervate at optimal mass ratio determinate from ζ-potential measurement. In order to measure the turbidity in terms of light absorption, a UV/Vis spectrophotometer model VE-5600UV (Científica Vela Quin S.A. de C.V., Mexico City, Mexico) used. The absorbance was measured at 236 nm at 25 °C and pH range in the complex coacervate WPI-Y was adjusted from 2.0 to 6.0 using HCl or NaOH solution (0.1 M). The optimal pH_{opt} corresponds to the value at which the highest optical density at 236 nm was observed.

2.5. Spray-drying of complex coacervate

Complex coacervates can be stored for subsequent applications in, e.g., dough matrices. Dried complexes have reduced water activity, and hence more stable shelf life. Solutions of complex coacervates containing 10% and 20% w/w of total solids content using MD as wall material were prepared. The yeasts count of WPI-Y complex coacervate and MD solutions was about 9×10^7 CFU/g. The solution was dried in a pilot scale spray-dryer Nichols/Niro (Turbo Spray PLA, NY, USA) with diameter drying chamber of 70 cm, diameter cyclone of 13 cm and air atomizing spray nozzle with air and liquid independent inlets at the back of the nozzle body in line with the spray direction. The solution was fed to the spray-dryer using a flow rate of 40 mL min^{-1} at 25 °C through a dispenser. The inlet and outlet temperatures were 150 °C and 80 °C, respectively, injecting a flow rate of drying air of 3.68 mL min^{-1} at 4 bar and absolute humidity of 10.95 kg air/dry air. Dry powders were placed and stored in airtight plastic containers at 25 °C until use. The resulting spray-dried WPI-Y complex coacervates were coded as $(WPI\text{-}Y)_c$, where c = the concentration of MD.

2.6. Differential scanning calorimetry (DSC)

The thermal stability of complex coacervates plays a central role in several applications where thermal processing is involved. DSC experiments were conducted to Y and $(WPI\text{-}Y)_c$ complex coacervates using a differential scanning calorimeter (DSC) model 204 F1 Phoenix (NETZSCH-Gerätebau GmbH, Selb, Germany) calibrated with indium. To avoid water condensation, nitrogen gas was

continuously flushed through the calorimeter head at a rate of 100 mL min^{-1}. Samples (4–5 mg) were placed in a hermetic sealed aluminum pan, which was placed inside the calorimeter and frozen to a temperature of −40 °C. Samples were subsequently heated to 150 °C with heating rate of 5.0 °C min^{-1}. An identical empty pan was used as reference. The temperature (T_d, °C) and enthalpy (ΔH, J g^{-1}) of denaturation were calculated by NETZSCH Proteus software provided by the manufacturer.

2.7. Freezing process of Y and spray-dried WPI-Y complex coacervates

Commonly, yeast and dough for bread making are stored under freezing conditions. Under freezing, the survival of yeast units might be affected by frozen water, reducing shelf life. Microencapsulation can be used for improving the viability of yeast in the face of freezing conditions. To assess the stability of Y and $(WPI\text{-}Y)_c$ complex coacervates were frozen (−10 C/min) in an air blast freezer model BK-5 (Tecnomac, Castel MAC SpA, Castelfranco Veneto, Italy) with air temperature in convection at −40 °C for 20 min until the temperature of powders reached −18 °C. After frozen, powders were transferred to airtight plastic containers and stored at −18 °C in a refrigerator until the moment of thawed for analysis after 24 h. Y and spray-dried $(WPI\text{-}Y)_c$ complex coacervates after freezing process were coded as Y_f and $(WPI\text{-}Y)_{cf}$, where f = samples after freezing process.

2.8. Fourier Transform Infrared spectroscopy

FTIR is a commonly used analysis to assess the interaction between materials involved in complex coacervation. A Bruker spectrophotometer (Alpha T, Bruker Optics Inc., Billerica, MA, USA) coupled to a crystal diamond universal ATR sampling accessory was used to obtain spectra of Fourier Transform Infrared (FTIR) of WPI, Y, Y_f, MD, $(WPI\text{-}Y)_c$ and $(WPI\text{-}Y)_{cf}$ complex coacervates. A spectrum of the empty cell was used as background. The FTIR spectra were represented average of 32 scans in a range of 4000 to 400 cm^{-1} at a resolution of 4 cm^{-1}.

2.9. Scanning electron microscopy (SEM)

The morphology of complex coacervates was evaluated to gain insights in the possible formation of unstable wall material structures (e.g., fractures). WPI, Y, Y_f, MD, $(WPI\text{-}Y)_c$ and $(WPI\text{-}Y)_{cf}$ complex coacervates were attached to a sample circular aluminum stub with double-sided adhesive carbon tape. Then, samples were sputter coated with 15 nm of gold and examined using a scanning electron microscope (JEOL JSM 6380 LV, Jeol Ltd., Akishima, Japan) at an accelerating voltage of 5 kV. Micrographs at 2000× magnification were used for illustration purposes.

2.10. Yeast survival

Finally, complex coacervation is intended to improve the yeast survival in the face of adverse conditions. The yeast survival was determined by plate count method in Y, Y_f, $(WPI\text{-}Y)_c$ and $(WPI\text{-}Y)_{cf}$ complex coacervates. To this end, 1 g of powder was suspended in 99 mL of sterile saline peptone water solution (0.1% w/v), mixed and diluted as required. The hydrated sample of 1.0 mL were taken and spread onto potato dextrose agar plates as a culture media and incubated at 25 °C for 5–7 days. Yeast colonies (CFU/g) were counted and the mean value was used to assess the yeast survival.

2.11. Statistical analysis

All experiments were performed on triplicate samples and values were expressed as mean values ± SD. Statistical analysis was done through the program SPSS Statistics 19.0. To determine the statistically significant difference between values, analysis of variance one-way (ANOVA) and Tukey's test were performed. Differences were considered statistically significant at $P \leq 0.05$.

3. Results and discussion

3.1. Effects of pH on zeta potential of WPI, Y and WPI-Y complex coacervate formation

Before assessing the viability of Y, the properties of the formed coacervate with WPI were evaluated. The pH-dependent surface charge obtained from zeta potential measurements of the solutions of WPI, Y, and WPI-Y complex coacervate is shown in Fig. 1. The solution of WPI presented cationic character below its isoelectric point pH = 4.2 (Fig. 1a). For all pH values above isoelectric point, the WPI solution increased gradually its anionic character. The WPI solution presented the maximum cationic character for zeta

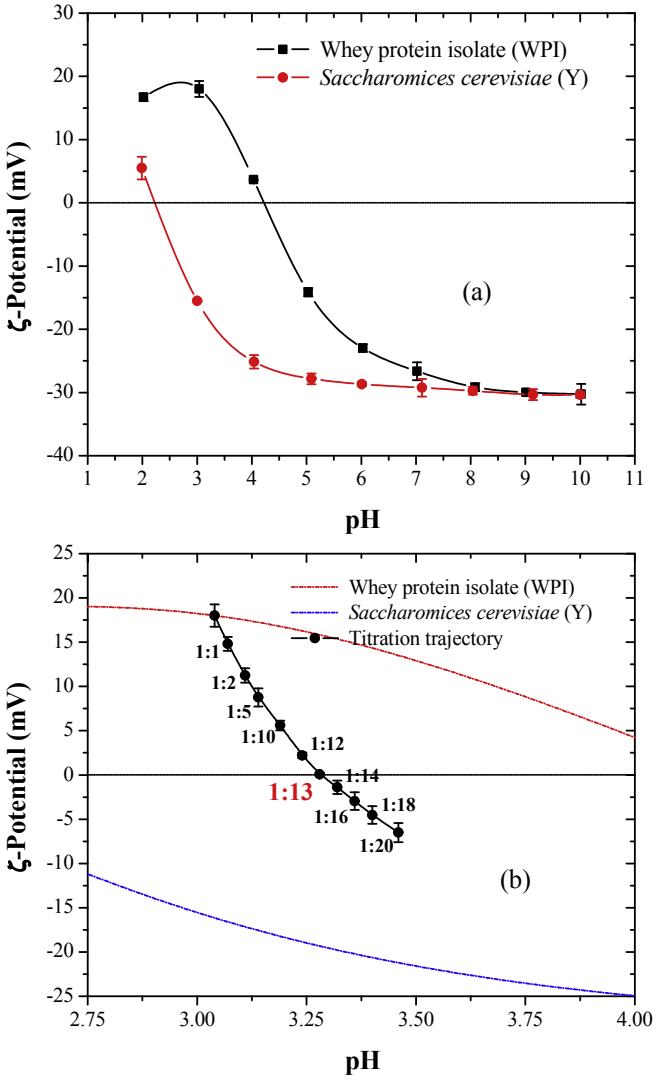

Fig. 1. (a) Zeta potential curves of WPI and Y solutions, and (b) Titration trajectory of WPI-Y complex coacervate on the zeta potential as a function of pH.

potential value of +18.01 mV at pH = 3.0. The pH dependence of zeta potential of WPI can be explained from the amphoteric character of proteins as they contain both amino (NH_2) and carboxyl (-COOH) functional groups. In fact, the increase in the zeta potential value could be attributed to the increasing number of positively charged amino groups ($-NH_3^+$), while many carboxyl groups in the system were neutralized ($-COO^-$) due to the deprotonation, as the pH decreased (Yuan, Kong, Sun, Zeng, & Yang, 2017). On the other hand, the solution of Y exhibited an anionic character for most of pH range studied. When the pH was reduced to 2.21, the zeta potential of the Y solution became slightly cationic due to the low pKa values (1.8–2.2) of carboxyl groups (-COOH) present in Y (Borchani et al., 2016; Timilsena, Wang, Adhikari, & Adhikari, 2016). As shown in Fig. 1a, the anionic character decreased with increase in pH from 2.0 to 10.0 and the maximum anionic value of Y was −30.37 at pH = 10.0.

The trajectory of titration curve of the WPI-Y complex coacervate at different mass ratios is presented in Fig. 1b. The zeta potential for WPI-Y complex coacervate changed from positive to negative as the concentrations of Y increased. For low WPI-Y mass ratio, the positively charged WPI dominated the value of zeta potential, indicating that the excess of WPI macromolecules was unable to form complexes with the Y macromolecules, which remained in the soluble form in the equilibrium phase. However, the ratio located at the critical region (1:13 and pH = 3.27) was the maximum and occurred when the two oppositely charged materials presented a strong electrostatic attraction with each other and induced the charges neutralization (zero zeta potential), resulting in the decrease of electrostatic repulsive force of the WPI-Y complex coacervate. As the fraction of Y increased, the negative trend continued with the decrease of the zeta potential. These results are in agreement with early works (Eratte, Wang, Dowling, Barrow, & Adhikari, 2014; Liu, Shim, Shen, Wang, & Reaney, 2017) reporting that anionic materials (e.g., gum Arabic, flaxseed gum) can neutralize cationic WPI to form complex coacervates as a function of mass ratios. The results exhibited in Fig. 1 showed that Y has the ability of forming complex coacervates with WPI, a structure that can be exploited to improve the viability of yeast in the face of adverse environmental conditions (e.g., freezing). Overall, the results have shown that the optimum WPI-Y complex coacervate reached the best interaction for a ratio and pH of 1:13 and 3.28, respectively.

3.2. Determination of optimal pH of WPI-Y complex coacervate by turbidity

The formation of complex coacervates is strongly affected by the hydrogen ion conditions in solution. Electrostatic charges from the cationic material are likely to be neutralized by anionic charges of the opposite material. In this way, optimal pH conditions for achieving maximum production of complex coacervate can be estimated by means of turbidity measurements. Indeed, the optimal pH values corresponds with the optimal mass ratio determined by ζ-potential measurements. The sequential transition of phases observed by turbidimetric titrations of the WPI-Y complex coacervate are shown in Fig. 2. The first transition was detected for pH values of about 4.82 (pH_c), which corresponds to the formation of primary complex. In this phase, the solutions were transparent since the involved macromolecules have the same net charge that prevented any interaction or complex formation. Subsequently, the turbidity continued increasing until a pH value of 4.24 ($pH_{\varphi 1}$). At this point, the dispersion exhibited a quasi-neutralized insoluble complex linked to nucleation and growth of primary soluble complexes with no phase separation. As the pH decreased to value of about 3.28, the turbidity increased abruptly, displaying the

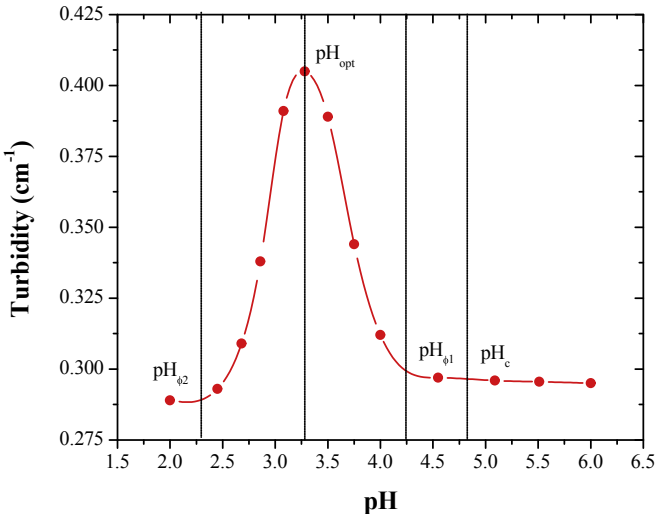

Fig. 2. Turbidity values as a function of pH for WPI-Y complex coacervate.

maximum interaction point (pH_{opt}) of the WPI-Y complexes. This phase corresponds to the formation of insoluble complexes with charges neutralization and cloudy solution. However, these complexes become unstable since phase separation was clearly observed. The value of pH_{opt} was in line with that obtained by zeta potential measurements (pH = 3.27). Finally, the turbidity of the WPI-Y complex coacervate decreased to pH of 2.29 ($pH_{\varphi 2}$), indicating the total disassociation of the complex coacervate as demonstrated by the solubility of the materials with translucent solution (Duhoranimana et al., 2017; Joshi, Rawat, & Bohidar, 2018). That is, complex coacervation between WPI and yeast is achieved for relatively acid hydrogen potentials, an effect induced maybe by hydrogenation of the WPI structure.

3.3. Thermal transitions of Y and spray-dried WPI-Y complex coacervates

The thermal stability of the spray-dried complex coacervate is of prime importance for certain applications, including bread making where baking takes place at relatively high temperatures (about 180–220 °C). The thermograms of Y and spray-dried WPI-Y

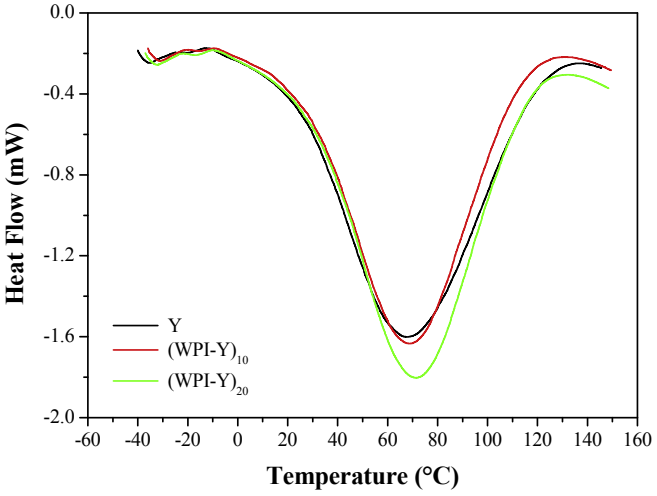

Fig. 3. Differential scanning calorimetric (DSC) thermograms of Y and spray dried WPI-Y complex coacervates.

complex coacervates obtained from DSC are presented in Fig. 3. The endothermic peak of the powders can be associated with the peak of denaturation temperature (T_d) of proteins (Table 1). The slight increase in T_d of the complex coacervates with respect to Y could be associated with a molecular rearrangement of the proteins from the Y, which eventually leads to improving the molecular interactions linked to the resistance of proteins to ice crystals formation (Pan & Wu, 2014). In fact, higher concentration of wall material in the spray-dried complex coacervates presented a higher denaturation temperature (Table 1).

The denaturation enthalpy (ΔH), defined as the amount of energy required to degrade the native structure of protein, was 15.25 J g^{-1}, 18.20 J g^{-1} and 23.07 J g^{-1}, for Y, $(WPI\text{-}Y)_{10}$ and $(WPI\text{-}Y)_{20}$, respectively (Table 1). Results indicated that the denaturation of the proteins in the complex coacervates required higher energy as compared to pure Y. This means that the $(WPI\text{-}Y)_{20}$ complex coacervate promoted the best thermal stability of the proteins after the freezing process. These results are in agreement with reported in previous studies (Chang, Gupta, Timilsena, & Adhikari, 2016; Duhoranimana et al., 2017), which showed that complex coacervation improves thermal stability of biomaterials.

3.4. FTIR of pure materials and spray-dried WPI-Y complex coacervates

Coacervation is possible thanks to the interactions between WPI, Y proteins and MD. Electrostatic interactions can be detected as these are able of modifying the molecular dynamics of coacervate matter. FTIR is a useful tool to detect binding interactions that can be interpreted as the formation of coacervates. WPI, Y, Y_f, MD, $(WPI\text{-}Y)_c$ and $(WPI\text{-}Y)_{cf}$ complex coacervates spectra of FTIR are shown in Fig. 4. The FTIR spectra were divided in three characteristic regions (3700-2800, 1800-1200 and 1200-800 cm^{-1}) and interpreted the absorption bands of the $(WPI\text{-}Y)_c$ and $(WPI\text{-}Y)_{cf}$ complex coacervates as function of the pure materials. In general, $(WPI\text{-}Y)_c$ and $(WPI\text{-}Y)_{cf}$ complex coacervates exhibited a similar behavior that the Y, with the only differences observed in the intensity of the peaks.

Table 1
Thermal transitions of Y and spray-dried WPI-SC complex coacervates.

Samples	T_d (°C)	ΔH (J g^{-1})
Y	67.87 ± 1.02^a	15.25 ± 0.23^a
$(WPI\text{-}Y)_{10}$	69.10 ± 1.17^a	18.20 ± 0.31^b
$(WPI\text{-}Y)_{20}$	71.61 ± 1.29^b	23.07 ± 0.44^c

Values are means ± standard error, of three replicates. Superscripts with different letters in same column indicate significant differences ($P \leq 0.05$).

3.4.1. Region I (3700-2800 cm^{-1})

In this region (Fig. 4a), the wide absorbance band at 3700-3000 cm^{-1} displayed peaks corresponding to vibrations of free, inter and intramolecular hydroxyl (-OH) groups. The peak at 3070 cm^{-1} for WPI was attributed to the amide B (Burgardt et al., 2014). Results depicted an upshift of OH-stretching band position with the increase of the concentration of MD due to the alteration of the hydrogen bonding. On the other hand, as the concentration of MD increase in the complex coacervate, the moisture content increased due to the hygroscopicity that present of wall material. Thus, the -OH stretching band depicted an important upshift (Sritham & Gunasekaran, 2017).

The bands in the range of 3000-2800 cm^{-1} represent absorptions ascribed to the stretching of the C-H corresponding to aliphatic groups. Peaks in this region (3000-2800 cm^{-1}) are assigned to the lipids of the plasmatic membrane for the Y (Burattini et al., 2008). The intensity of aliphatic groups was higher with the concentration of MD and after freezing process in comparison with the bands presented by Y. These differences could be related to the contribution of the vibrations of WPI. The opposite tendency was observed for Y respect to the complex coacervates, which displayed a downshift behavior of the -OH stretching vibrations in both regions (3700-3000 cm^{-1} and 3000-2800 cm^{-1}). This effect could be due to the biochemical changes resulting from the disorganization of the plasmatic membrane and modification on the length of lipid chains (Adt, Toubas, Pinon, Manfait, & Sockalingum, 2006).

3.4.2. Region II (1800-1200 cm^{-1})

The main characteristic bands in this region are ascribed of the Amide I, II and III of WPI and Y. Amide I and Amide II groups correspond to C=O, N-H and C-N stretching vibrations, respectively, which are characteristic of the proteins and peptides. A wide absorption band in the range of 1200–1500 cm^{-1} (Amide III) depict an overtone vibration of N-H bending and C-N stretching of amide bonds and the vibration wagging of the CH_2 groups. Bands in this region for MD are related to the C-H and CH_3 bendings. The spray-dried WPI-Y complex coacervates exhibited upshift in the amide groups as the concentration was increased compared to the Y due to the amino groups of Y and WPI interact with the carboxyl groups of MD to form a complex containing an amide bond. In contrast, after the freezing process, complex coacervates presented downshift in the bands intensity, suggesting partially degraded proteins to an unfolded and disorganized state (Paramera, Konteles, & Karathanos, 2011). This observation is in accordance with the DSC

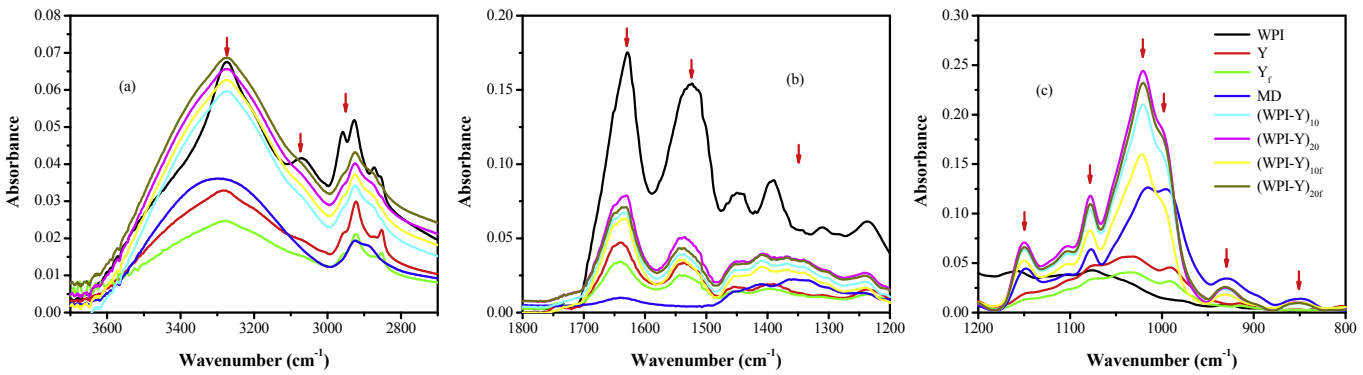

Fig. 4. FTIR spectra of the pure materials and spray-dried WPI-Y complex coacervates divided in three characteristic regions: (a) Region I (3700-2800 cm^{-1}), (b) Region II (1800-1200 cm^{-1}), and (c) Region III (1200-800 cm^{-1}).

results, where the proteins denaturation was displayed when the complex coacervates were frozen. In turn, this effect confirms the degradation of one part of yeast proteins in peptides and amino-acids, mainly involving the cell membrane and the cell wall.

3.4.3. Region III (1200-800 cm^{-1})

The characteristic absorption bands commonly in carbohydrates can be found in this region, corresponding to the C-O-C symmetric stretching absorption and C-O stretching group for WPI and MD (Jain, Thakur, Ghoshal, Katare, & Shivhare, 2015). For the sample Y, the bands located in the cell wall correspond to β-glucans, glycogen and mannans (Borchani et al., 2016). The intensity of absorption bands in this region increased in the complex coacervates when MD concentration increased, suggesting the strengthening of glycosidic linkages due to that galacturonic acid present in MD not participates in the complex formation. Otherwise, a decrease in the absorption bands was exhibited by complex coacervates and Y after freezing process, indicating that the glycosidic linkages was hydrolyzed. It has been point out that plasmolysed cells induces the degradation of polysaccharide yeast cells (Kaushik, Dowling, McKnight, Barrow, & Adhikari, 2016).

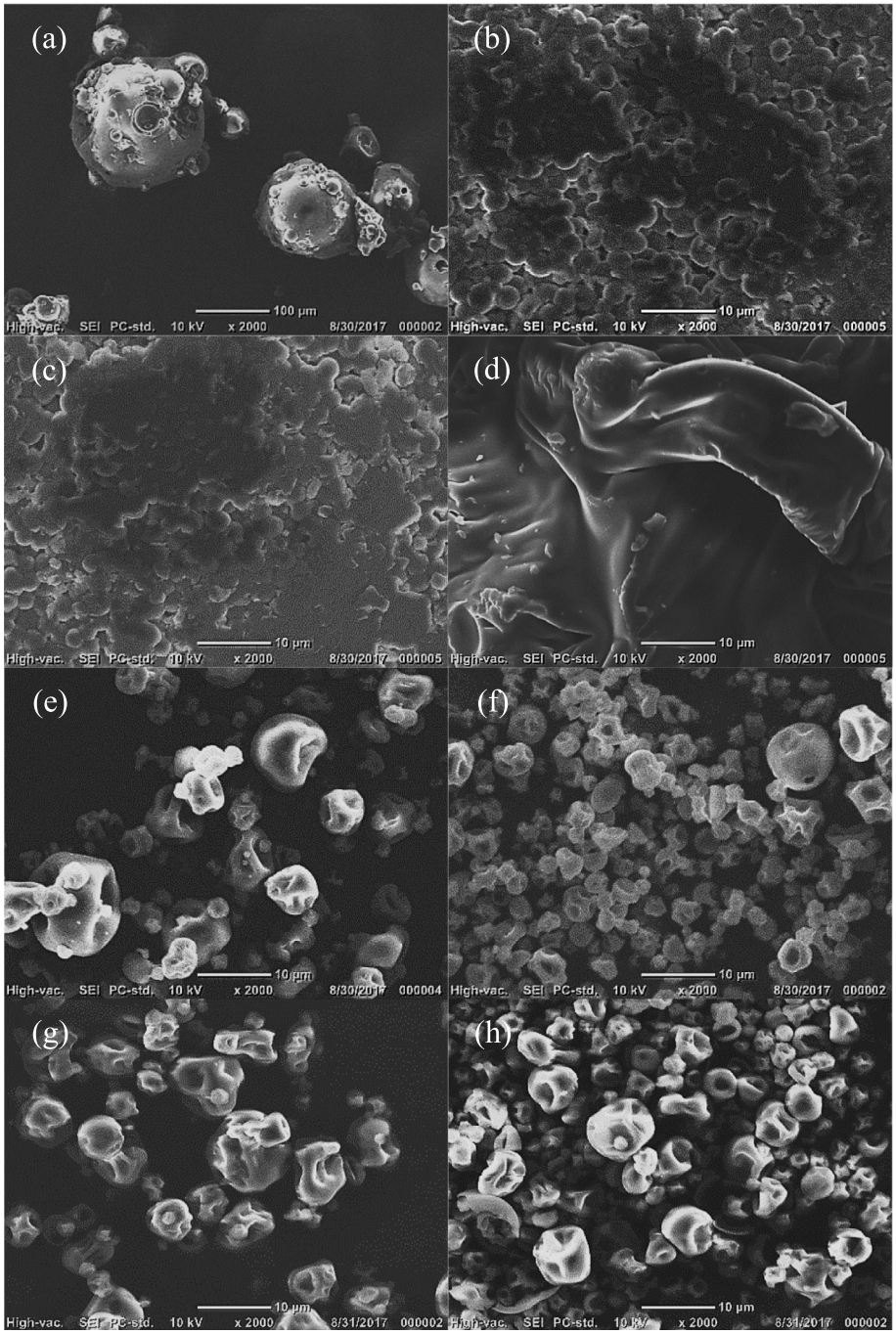

Fig. 5. SEM micrographs of: (a) WPI, (b) Y, (c) Y_f, (d) MD, (e) spray-dried $(WPI\text{-}Y)_{10}$ complex coacervate, (f) spray-dried $(WPI\text{-}Y)_{20}$ complex coacervate, (g) spray-dried $(WPI\text{-}Y)_{10f}$ complex coacervate, and (h) spray-dried $(WPI\text{-}Y)_{20f}$ complex coacervate.

3.5. Morphology of pure materials and spray-dried WPI-Y complex coacervates

The morphology of individual materials and the formed coacervate can provide valuable insights in the stability of encapsulated Y. Fig. 5 shows the SEM images of the pure materials, $(WPI\text{-}Y)_c$ and $(WPI\text{-}Y)_{cf}$ complex coacervates. The outer topography of WPI and Y (Fig. 5a and b) exhibited spherical shape particles with surface dents and smooth particles like bubbles, respectively, free of visible fractures and pores on the surface (Ahmad, Kausmann, Imtiaz-ul-Islam, & Langrish, 2013; Sultana et al., 2017). However, freezing process affected the Y particles, resulting in a slight destruction of the original structures due to the water adsorbed in the surface (Fig. 5c). The micrographs of MD revealed (Fig. 5d) amorphous and irregular forms with flat regions in the surface.

The $(WPI\text{-}Y)_c$ complex coacervates exhibited spherical shapes with concavities and dents without levels of breakage on the surface, due to rapid shrinkage of the droplets of the complex coacervate solutions during the early stage of the drying process. In addition, the greater amount of particles displayed holes at the center, which can be related to the expansion of the particles during the latter stages of the drying process (Amara, Eghbal, Degraeve, & Gharsallaoui, 2016). The powder size of $(WPI\text{-}Y)_c$ complex coacervates was found within a range of 2–10 μm. As the concentration of MD increased, more uniform sized and small particles can be observed (Fig. 5e and f). On the other side, the presence of fractures in the particles of the $(WPI\text{-}Y)_{cf}$ complex coacervates (Fig. 5g and h) were associated to swelling and at size increase of the particles during freezing process because of the adsorption of water. Further, these irregularities are closely related to the water evaporation rate during the thawed process (Sanchez-Reinoso, Osorio, & Herrera, 2017). The microstructure of the complex coacervate suggests that MD reduced irregularities, leading to homogeneous material for yeast protection.

3.6. Survival of Y and spray-dried WPI-Y complex coacervates

The main focus of this study was on the survival of yeast units embedded into the coacervation system. The count of colonies formation units of Y and spray-dried WPI-Y complex coacervates are shown in Table 2. After the freezing process, yeast number of Y decreased ($25.00\ CFU/g \times 10^7$) with respect to the original number of colonies ($30.00\ CFU/g \times 10^7$) since the plasmatic membrane of the cells are broken, producing partial inactivation and death of Y. The dispersion and protection of yeast colonies in complex coacervated material can lead to viability improving. In fact, results from zeta potential studies showed that opposite-charge electrostratic effects between Y and WPI allowed the formation of complex coacervates between these two components. To assess this point, $9.00\ CFU/g \times 10^7$ number of colonies was used for microencapsulation of the yeast cells of Y by complex coacervation in order to protect the initial number of colonies after freezing process. Complex coacervation was effective for reducing the death of yeast colonies, an effect ascribed to binds formed between Y components and WPI as characterized by FTIR analysis (see Fig. 4). It can be suggested that bindings plays the role of anti-freezing agent, reducing the adverse effects of ice formation during the freezing process (Griffith & Ewart, 1995). In turn, anti-freezing effect would lead to reduced number of yeast units death. As can be seen in Table 2, a higher number of colonies were obtained when the concentration of MD increased in the complex coacervate, showing relatively low death of initial inoculums after freezing process ($7.00\ CFU/g \times 10^7$) with respect to the less concentration of MD. This behavior can be related to a reduction of effects of the temperature during the spray-drying process and with water transfer to the inner of the microcapsules when the concentration of MD increased (Arslan, Erbas, Tontul, & Topuz, 2015). Morphology characterization (Fig. 5e and f) showed that more homogeneous sizes and small particles can be obtained with the addition of MD. The reduction of micro-fractures and cavities led to improved protection of yeast units. Chandralekha et al. (2016) also studied the effect of different carrier materials to encapsulate yeast cells of *Saccharomyces cerevisiae* by spray-drying and freeze-drying on their survival during the storage time, flow properties, morphology and particle size. It was concluded that yeast cells displayed a higher protection during storage time when using a combination of whey protein and corn starch as carrier material by spray-drying. The results in the present study showed that coacervation-mediated protection is a viable alternative for enlarging the survival rate of yeast for applications under, e.g., freezing conditions.

Table 2
Yeast count of SC and spray-dried WPI-Y complex coacervates.

Samples	Yeast count $(CFU/g) \times 10^7$
Y	30.00 ± 0.60^{g}
Y_f	25.00 ± 0.53^{f}
WPI-Y	9.00 ± 0.16^{e}
$(WPI\text{-}Y)_{10}$	5.00 ± 0.09^{b}
$(WPI\text{-}Y)_{20}$	8.00 ± 0.12^{d}
$(WPI\text{-}Y)_{10f}$	3.00 ± 0.07^{a}
$(WPI\text{-}Y)_{20f}$	7.00 ± 0.10^{c}

Values are means ± standard error, of three replicates. Superscripts with different letters in same column indicate significant differences ($P \leq 0.05$).

4. Conclusions

The present study showed enhancement in the protection of the yeast cells of Y using spray-dried WPI-Y complex coacervates with 10% and 20% w/w of MD as wall material and after the freezing process. The spray-dried $(WPI\text{-}Y)_{20}$ complex coacervate resulted in better protection of the yeast cells of Y after the freezing process compared to spray-dried $(WPI\text{-}Y)_{10}$ complex coacervate. The DSC analysis exhibited higher denaturation peak temperature and enthalpy as concentration of MD increased. These results were confirmed with the FTIR analysis since the peaks intensity of the amides increased with the incorporation of MD. SEM images of spray-dried complex coacervates displayed spherical irregular shapes and after freezing process some particles showed fractures. Thus, an alternative to protect yeast cells of Y against adverse effects of freezing process is to form complex coacervates with WPI by spray-drying using MD as wall material.

Acknowledgements

The authors wish to thank the financial support provided by Universidad Autónoma del Estado de México through of the project "Encapsulación de levadura para prolongar su viabilidad en la producción y almacenamiento de masas ultracongeladas" with key project number 4544/2018/CI.

Nomenclature

DSC	Differential scanning calorimetry
FTIR	Fourier transform infrared spectroscopy
MD	Maltodextrin
WPI	Whey protein isolate
$(WPI\text{-}Y)_c$	WPI and Y complex coacervate with MD concentration
Y	Yeast (*Saccharomyces cerevisiae*)

Conflicts of interest

The authors declare no conflict of interest.

References

Adt, I., Toubas, D., Pinon, J. M., Manfait, M., & Sockalingum, G. D. (2006). FTIR spectroscopy as a potential tool to analyse structural modifications during morphogenesis of *Candida albicans*. *Archives of Microbiology, 185*(4), 277–285.

Ahmad, J., Kausmann, T., Imtiaz-ul-Islam, M., & Langrish, T. A. G. (2013). The effect of fats in whey protein isolate powder. *Drying Technology, 31*(6), 619–632.

Amara, C. B., Eghbal, N., Degraeve, P., & Gharsallaoui, A. (2016). Using complex coacervation for lysozyme encapsulation by spray-drying. *Journal of Food Engineering, 183*, 50–57.

Arslan, S., Erbas, M., Tontul, I., & Topuz, A. (2015). Microencapsulation of probiotic Saccharomyces cerevisiae var. boulardii with different wall materials by spray drying. *LWT-Food Science and Technology, 63*(1), 685–690.

Borchani, C., Fonteyn, F., Jamin, G., Paquot, M., Thonart, P., & Blecker, C. (2016). Physical, functional and structural characterization of the cell wall fractions from baker's yeast *Saccharomyces cerevisiae*. *Food Chemistry, 194*, 1149–1155.

Bosnea, L. A., Moschakis, T., & Biliaderis, C. G. (2017). Microencapsulated cells of *Lactobacillus paracasei* subsp. *paracasei* in biopolymer complex coacervates and their function in a yogurt matrix. *Food & Function, 8*(2), 554–562.

Bot, A. (2003). Differential scanning calorimetric study on the effects of frozen storage on gluten and dough. *Cereal Chemistry, 80*(4), 366–370.

Burattini, E., Cavagna, M., Dell'Anna, R., Malvezzi Campeggi, F., Monti, F., Rossi, F., et al. (2008). A FTIR microspectroscopy study of autolysis in cells of the wine yeast *Saccharomyces cerevisiae*. *Vibrational Spectroscopy, 47*(2), 139–147.

Burgardt, V. C. F., Oliveira, D. F., Evseev, I. G., Coelho, A. R., Haminiuk, C. W. I., & Waszczynskyj, N. (2014). Influence of concentration and pH in casein-omacropeptide and carboxymethylcellulose interaction. *Food Hydrocolloids, 35*, 170–180.

Chandralekha, A., Tavanandi, A. H., Amrutha, N., Hebbar, H. U., Raghavarao, K. S. M. S., & Gadre, R. (2016). Encapsulation of yeast (*Saccharomyces cereviciae*) by spray drying for extension of shelf life. *Drying Technology, 34*(11), 1307–1318.

Chang, P. G., Gupta, R., Timilsena, Y. P., & Adhikari, B. (2016). Optimisation of the complex coacervation between canola protein isolate and chitosan. *Journal of Food Engineering, 191*, 58–66.

Duhoranimana, E., Karangwa, E., Lai, L., Xu, X., Yu, J., Xia, S., et al. (2017). Effect of sodium carboxymethyl cellulose on complex coacervates formation with gelatin: Coacervates characterization, stabilization and formation mechanism. *Food Hydrocolloids, 69*, 111–120.

Eghbal, N., & Choudhary, R. (2018). Complex coacervation: Encapsulation and controlled release of active agents in food systems. *LWT-Food Science and Technology, 90*, 254–264.

Eratte, D., Wang, B., Dowling, K., Barrow, C. J., & Adhikari, B. P. (2014). Complex coacervation with whey protein isolate and gum Arabic for the microencapsulation of omega-3 rich tuna oil. *Food & Function, 5*(11), 2743–2750.

Giannou, V., Kessoglou, V., & Tzia, C. (2003). Quality and safety characteristics of bread made from frozen dough. *Trends in Food Science & Technology, 14*(3), 99–108.

Griffith, M., & Ewart, K. V. (1995). Antifreeze proteins and their potential use in frozen foods. *Biotechnology Advances, 13*(3), 375–402.

Jain, A., Thakur, D., Ghoshal, G., Katare, O. P., & Shivhare, U. S. (2015). Microencapsulation by complex coacervation using whey protein isolates and gum acacia: An approach to preserve the functionality and controlled release of β-carotene. *Food and Bioprocess Technology, 8*(8), 1635–1644.

Joshi, N., Rawat, K., & Bohidar, H. B. (2018). pH and Ionic strength induced complex coacervation of Pectin and Gelatin A. *Food Hydrocolloids, 74*, 132–138.

Kaushik, P., Dowling, K., McKnight, S., Barrow, C. J., & Adhikari, B. (2016). Microencapsulation of flaxseed oil in flaxseed protein and flaxseed gum complex coacervates. *Food Research International, 86*, 1–8.

Keen, P. H., Slater, N. K., & Routh, A. F. (2011). Encapsulation of yeast cells in colloidosomes. *Langmuir, 28*(2), 1169–1174.

Kim, Y. S., Huang, W., Du, G., Pan, Z., & Chung, O. (2008). Effects of trehalose, transglutaminase, and gum on rheological, fermentation, and baking properties of frozen dough. *Food Research International, 41*(9), 903–908.

Kondakci, T., Ang, A. M. Y., & Zhou, W. (2015). Impact of sodium alginate and xanthan gum on the quality of steamed bread made from frozen dough. *Cereal Chemistry, 92*(3), 236–245.

Liu, J., Shim, Y. Y., Shen, J., Wang, Y., & Reaney, M. J. (2017). Whey protein isolate and flaxseed (*Linum usitatissimum* L.) gum electrostatic coacervates: Turbidity and rheology. *Food Hydrocolloids, 64*, 18–27.

Matuda, T. G., Parra, D. F., Lugao, A. B., & Tadini, C. C. (2005). Influence of vegetable shortening and emulsifiers on the unfrozen water content and textural properties of frozen French bread dough. *LWT-Food Science and Technology, 38*(3), 275–280.

Pan, S., & Wu, S. (2014). Effect of chitooligosaccharides on the denaturation of weever myofibrillar protein during frozen storage. *International Journal of Biological Macromolecules, 65*, 549–552.

Paramera, E. I., Konteles, S. J., & Karathanos, V. T. (2011). Microencapsulation of curcumin in cells of *Saccharomyces cerevisiae*. *Food Chemistry, 125*(3), 892–902.

Poirier, I., Maréchal, P. A., Richard, S., & Gervais, P. (1999). *Saccharomyces cerevisiae* viability is strongly dependant on rehydration kinetics and the temperature of dried cells. *Journal of Applied Microbiology, 86*(1), 87–92.

Priya, A. J., Vijayalakshmi, S. P., & Raichur, A. M. (2011). Enhanced survival of probiotic Lactobacillus acidophilus by encapsulation with nanostructured polyelectrolyte layers through layer-by-layer approach. *Journal of Agricultural and Food Chemistry, 59*(21), 11838–11845.

Räsänen, J., Blanshard, J. M. V., Mitchell, J. R., Derbyshire, W., & Autio, K. (1998). Properties of frozen wheat doughs at subzero temperatures. *Journal of Cereal Science, 28*(1), 1–14.

Ribotta, P. D., Pérez, G. T., Leon, A. E., & Anon, M. C. (2004). Effect of emulsifier and guar gum on micro structural, rheological and baking performance of frozen bread dough. *Food Hydrocolloids, 18*(2), 305–313.

Rosell, C. M., & Gómez, M. (2007). Frozen dough and partially baked bread: An update. *Food Reviews International, 23*(3), 303–319.

Sanchez-Reinoso, Z., Osorio, C., & Herrera, A. (2017). Effect of microencapsulation by spray drying on cocoa aroma compounds and physicochemical characterisation of microencapsulates. *Powder Technology, 318*, 110–119.

Selomulyo, V. O., & Zhou, W. (2007). Frozen bread dough: Effects of freezing storage and dough improvers. *Journal of Cereal Science, 45*(1), 1–17.

Sritham, E., & Gunasekaran, S. (2017). FTIR spectroscopic evaluation of sucrose-maltodextrin-sodium citrate bioglass. *Food Hydrocolloids, 70*, 371–382.

Sultana, A., Miyamoto, A., Hy, Q. L., Tanaka, Y., Fushimi, Y., & Yoshii, H. (2017). Microencapsulation of flavors by spray drying using *Saccharomyces cerevisiae*. *Journal of Food Engineering, 199*, 36–41.

Timilsena, Y. P., Wang, B., Adhikari, R., & Adhikari, B. (2016). Preparation and characterization of chia seed protein isolate–chia seed gum complex coacervates. *Food Hydrocolloids, 52*, 554–563.

Timilsena, Y. P., Wang, B., Adhikari, R., & Adhikari, B. (2017). Advances in microencapsulation of polyunsaturated fatty acids (PUFAs)-rich plant oils using complex coacervation: A review. *Food Hydrocolloids, 69*, 369–381.

Yuan, Y., Kong, Z. Y., Sun, Y. E., Zeng, Q. Z., & Yang, X. Q. (2017). Complex coacervation of soy protein with chitosan: Constructing antioxidant microcapsule for algal oil delivery. *LWT-Food Science and Technology, 75*, 171–179.

Zhang, Y., Zhang, H., Wang, L., Qian, H., & Qi, X. (2015). Extraction of oat (*Avena sativa* L.) antifreeze proteins and evaluation of their effects on frozen dough and steamed bread. *Food and Bioprocess Technology, 8*(10), 2066–2075.

Đorđević, V., Balanč, B., Belščak-Cvitanović, A., Lević, S., Trifković, K., Kalušević, A., et al. (2015). Trends in encapsulation technologies for delivery of food bioactive compounds. *Food Engineering Reviews, 7*(4), 452–490.